

Microstructural Characterization and Wear Behavior of Varying Weight Percentages of Boron Carbide Reinforced Al2219 Alloy Composites

Subhashchandra S. Ganiger^{1*}, Mahadev Sakri¹, Madeva Nagara² and V. Auradi³

¹Department of Mechanical Engineering, B.L.D.E.A's Dr. P. G. Halakatti College of Engineering and Technology, Vijayapura - 586103, Karnataka, India; subbusg123@gmail.com

²Aircraft Research and Design Centre, HAL, Bangalore - 560037, Karnataka, India

³Department of Mechanical Engineering, Siddaganga Institute of Technology, Tumakuru - 572103, Karnataka, India

Abstract

The current study looked at how 90 micron-diameter B_4C particles affected the wear behavior of Al2219 metal composites. Stir-cast Al2219 composites with 2-4 % B_4C particle weight percentage were developed. The microstructural characterization of these generated composites was studied using SEM and EDS analysis to determine the distribution and components of micron-sized particles. Under different loads and sliding speeds, the wear behavior of Al2219 with 2-4 % B_4C composites was investigated using ASTM G99 criteria. The aggregation of B_4C concentration improved Al2219's wear resistance. The wear of Al2219 and its composites increased as the load and speed of the specimen increased. SEM investigation revealed several worn surface characteristics.

Keywords: Al2219 alloy, B_4C Particles, Stir Casting, Wear, Worn Morphology

1.0 Introduction

The most widely used framework materials for the creation of composites are still aluminum and its alloys^{1,2}. This is primarily because it offers a wide range of fascinating features at a comparatively low preparation cost. Among the desirably combinations of Al-based network composites are reduced warm extension, warm conductivity, high specific stiffness and strength, and exceptional high temperature properties^{3,4}.

It has been observed that these materials are utilized in the production of bearings, bushes, brakes, transmission belts, gears, and cams⁵. Tribological stacking conditions are applied to the components in the majority of these administrations. Although there are different ways to

fabricate MMC materials, there isn't any specific training for this topic. The kinds of materials used, along with the fortification and supports used, can significantly affect production tactics. Two categories of creation techniques exist. The liquid stage building method uses fluid metal invasion, stir casting, compo casting, and splash co-statement. While throwing courses, like blend throwing, and softening are by far the most sensible ways to prepare such Al-based composites, they are not without their drawbacks, which are mainly related to the density difference between the two materials and the obvious non-wettability of the particles by fluid aluminum compounds^{6,7}. Presenting and maintaining hard fired particles such as Al_2O_3 , B_4C , and TiC in liquid aluminum, as well as microscopic particles like graphite,

*Author for correspondence

in this way is quite challenging. Insufficient wettability and disparities in thickness also lead to insufficient graphite particle recovery during aluminum liquefaction. For free weight transfer and appropriation from the lattice to the fortifications, there must be sufficient wetness during throwing to provide enticing security between fluid metal and particle fortifications. The purpose of this study was to introduce particles into the framework in two stages in order to increase the wettability of aluminum fortification particles. B_4C is compatible with aluminum and establishes an excellent bond with the matrix between these reinforcements.

In this study, two and four weight percent of B_4C particles of a 90-micron size were added to the matrix using a novel two-stage reinforcement addition technique to create Al2219 composites. Using wear testing apparatus, the effects of load and sliding speed on the Al2219- B_4C composites' wear properties were further investigated.

2.0 Experiential Details

2.1 Materials Used

The foundational material was Al2219, and the reinforcement was micro- B_4C . Theoretical densities for

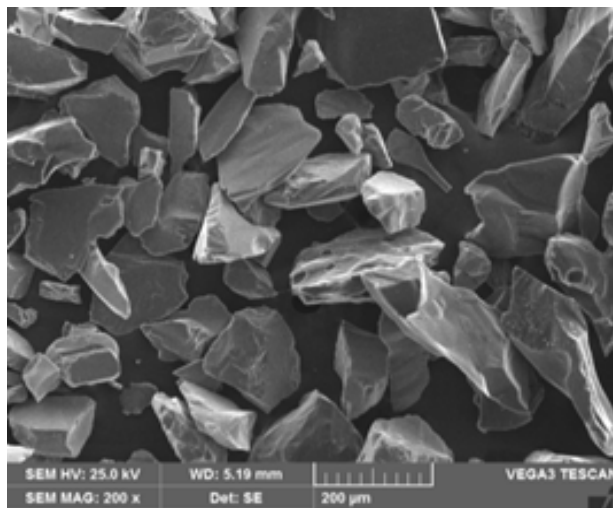


Figure 1. SEM of 90-micron sized B_4C .

Table 1. Chemistry of Al2219 alloy

Elements	Si	Fe	Cu	Mg	Zr	Zn	Ti	Mn	Al
Weight (%)	0.15	0.28	6.77	0.01	0.10	0.10	0.10	0.02	Bal

B_4C support particles and Al2219 amalgam grid material are 2.52 and 2.80 g/cm³, respectively. Table 1 displays the chemical composition of the Al2219 composite used in this research.

Micro B_4C of a size of 80 to 90 microns are used as fortification materials in the current study. B_4C has a lower density than the matrix material, which has a density of 2.52 g/cm³.

2.2 Preparation of Composites

Al2219- B_4C composites were produced using a stir casting method and a liquid metallurgical course, with an estimated particle size of 90 microns. In the furnace, a specific volume of Al2219 compound ingots is liquefied. Aluminum alloys have a melting point of 660°C. The temperature of the liquefied was raised to 750 degrees Celsius. A thermocouple made of chrome-alluminum will be used to record the temperature. Next, solid hexachloroethane (C_2Cl_6) is used to degas the liquid metal for three minutes. A vortex is created using a zirconium-coated tempered steel impeller. The impeller will be submerged to a depth of 60% of the liquid metal's height from the liquefied exterior while the stirrer spins at 300 rpm. Moreover, the B_4C particles will be heated in a heater to 500°C before to being added to the vortex. Stirring will go on until there is a moist condition in the interface communications between the network and the support particles. After that, the mixture containing Al2219-2 weight percent B_4C is put into a durable cast iron die. Similarly, 4% composition B_4C particle reinforced composites are made. In addition, based on microstructural analysis, wear qualities were tested for a range of loads, sliding speeds, and 3000 m sliding distance utilizing ASTM G99⁸ principles.

2.3 Wear Test

A wear test device was used to conduct dry sliding wear testing on Al2219 amalgam and Al2219- B_4C composites. On a stick holder, cylindrical examples with an 8 mm diameter and a 30 mm length were attached vertically.



Figure 2. Wear test specimen.

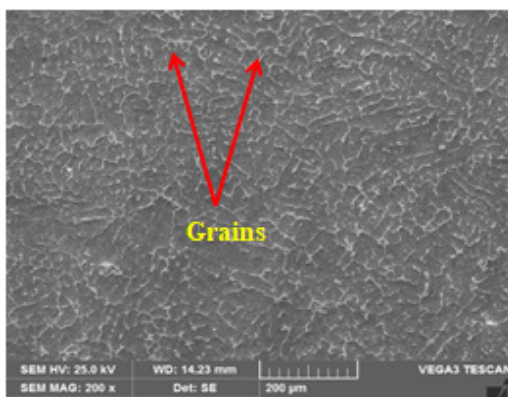
Throughout the evaluation, the pin was pressed up against a 60 HRC hardness EN32 steel plate. The steel counterface was first rough-ground with a 320-grit abrasive for a few minutes before being smoothed out with a 600-grit SiC abrasive and finally cleaned with acetone. The tests were conducted with variable speeds ranging from 100 to 400 rpm and typical loads ranging from 10 to 40 N at

400 rpm. The example's underlying load was calculated with 0.01mg precision in an electronic gauging machine. Information was obtained and recorded in order to reduce wear rates and weight. Figure 2 is a wear test specimen.

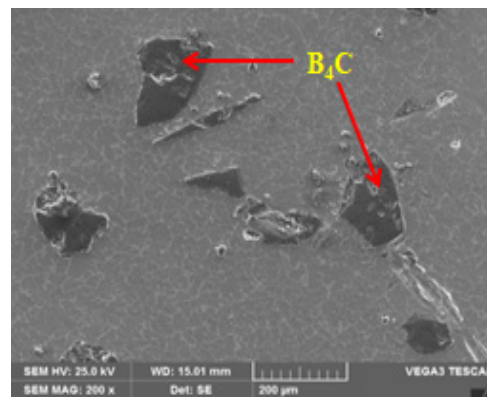
3.0 Results and Discussion

3.1 Microstructural Analysis

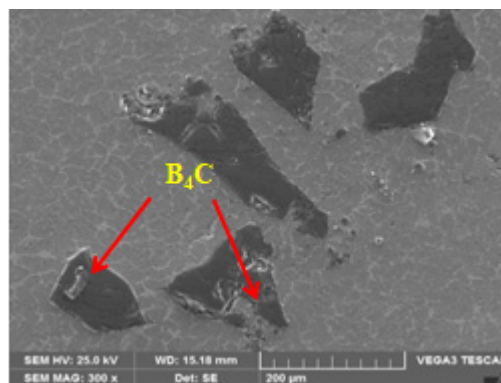
Figure 3(a) depicts the microstructure of a cast Al2219 aluminium alloy, while Figures 3(b-c) depicts Al2219 with 2, 4, and 4 % B_4C , respectively. As shown in Figures 3(b-c), SEM micrographs showed a very homogeneous distribution of B_4C particles throughout the matrix. Uniformly distributed particles improve the MMC's overall strength and other qualities while lowering its porosity.



(a)

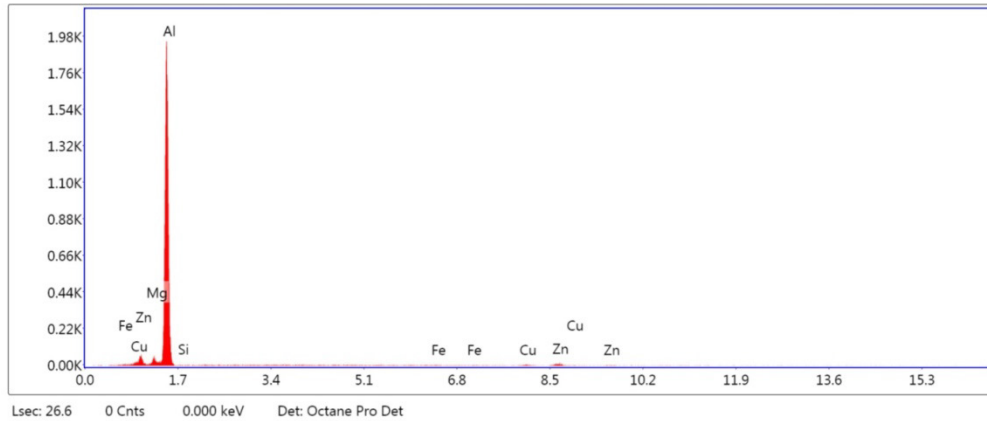


(b)

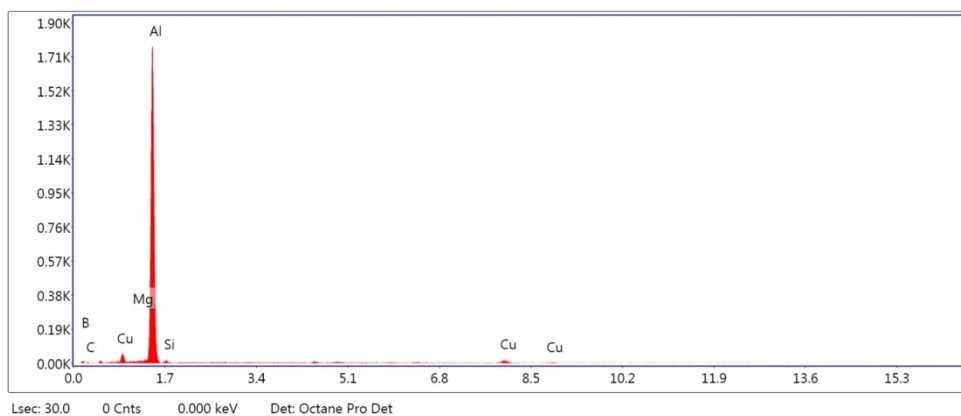


(c)

Figure 3. SEM images of (a) as cast Al2219 (b) Al2219 with 2% B_4C (c) Al2219 with 4% B_4C composites.



(a)



(b)

Figure 4. EDS of (a) Al2219 alloy (b) Al2219 with 4% B₄C composites.

The number of particles in the Al2219 alloy matrix increases, as seen in Figure 3(c). Furthermore, substantial interfacial adhesion between the B₄C particles and the Al2219 alloy matrix can be seen, indicating that the composites are strong.

The existence of B₄C is established by an energy dispersive spectroscopy investigation done on the B₄C and Al composites. The spectrum verifies the existence of Cu, Mg, Zn, B, and C in the Al2219 composites, as illustrated in Figures 4a and 4b.

3.2 Wear Behavior

Figure 5 depicts the wear loss range. The most essential factor influencing wear behavior is applied load, which has a significant impact on Al alloy and composite

material wear. Wear loss varies with normal load and is much lower for composite materials, according to Archard's law. Wear misfortune for network compounds and composites increases as applied loads increase. Nonetheless, in terms of wear obstruction, the composites outperform the framework compound at all loads. Several research^{9,10} shown that several wear indications could be discovered under various linked load scenarios, where MMC wear confrontation is more severe than Al2219 combination. The surface temperature rises above a fundamental value when independent wear and stresses increase. Wear increases with connection load for both alloys and composites. Figure 5 depicts the wear of grid amalgam Al2219 composites with 2 and 4 weight percent B₄C components. The increased hardness of composites

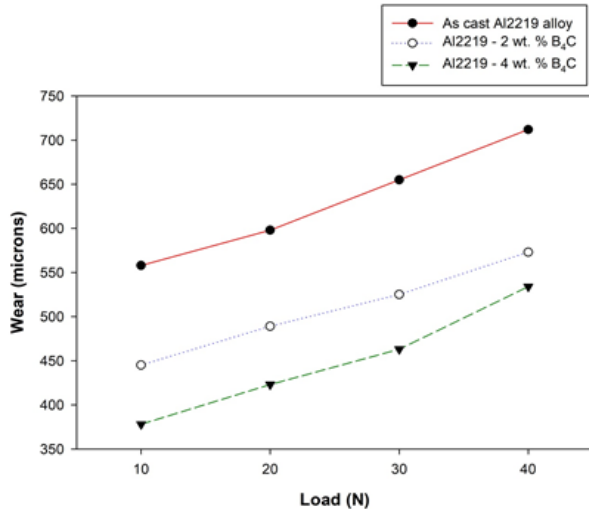


Figure 5. Wear of Al2219 and its composites.

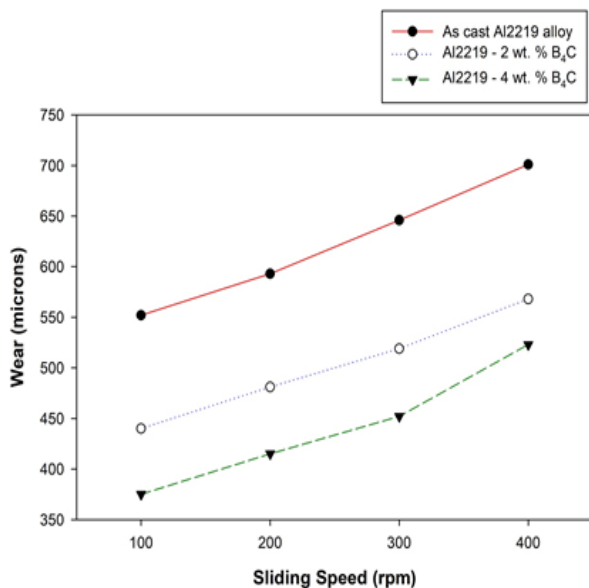


Figure 6. Wear of Al2219 Alloy and its composites at varying speeds.

fortified with B₄C results in a decrease in volumetric wear loss, which is responsible for the improvement in wear confrontation.

Figure 6 depicts the wear loss of an Al2219 compound and a 2 to 4 weight percent B₄C composite under different sliding velocities and a constant 40 N load. At higher rates, such as 100, 200, 300, and 400 rpm, both the matrix and its composites wear out. In any case, when connected to the network combination, the composite

wore much less for all sliding speeds considered. The increased heat of the composite is the reason for the faster wear rate with increased sliding speed¹¹. Nonetheless, increased temperature can cause visible plastic behavior of the mating surfaces at higher sliding speeds, resulting in increased wear. The enhanced rate of subsurface abnormalities shattering and fracturing angry tempers creates the contact zone. As a result, delamination improves, resulting in a higher wear rate.

3.3 Worn Morphology

The worn morphology of Al2219-B₄C composites is important for research because it reveals the types of wear that materials of varied compositions have endured. Since the Al2219 matrix is less substantial than the rubbing disc, it exhibits viscous flow; as the disc rubs against the pin-shaped Al matrix, plastic-like surface deformation and significant material loss result. Wear loss is facilitated by micro-pits and a fractured oxide layer on the Al2219's worn surface, as seen in Figure 7a. The matrix's viscous flow is restricted by B₄C particles¹². In the meantime, strain concentration develops around these B₄C particles (b-c), and stress appears to be transferred to them, as seen in Figure 7.

4.0 Conclusions

The present study's results on the preparation of liquefy melt and assessment of Al2219-B₄C metal grid composite are as follows. Combining the two-phase expansion technique for particle preheating and fortification with the melt stir approach allowed for the successful manufacture of composites based on the Al2219 combination. Al2219 amalgam metal framework composites' SEM microphotographs showed a constant flow of support particles. The wear resistance of the composite is increased by the expansion of B₄C particles into an Al2219 combination grid. There is more wear and tear than load factor and sliding rate. Increases in weight and sliding speed cause a significant rise in wear misfortune. When compared to a cast Al2219 amalgam grid, the wear misfortune rate is reduced in the Al2219-B₄C composites. SEM of worn surfaces revealed the close closeness of smooth portions in the Al2219-B₄C composite.

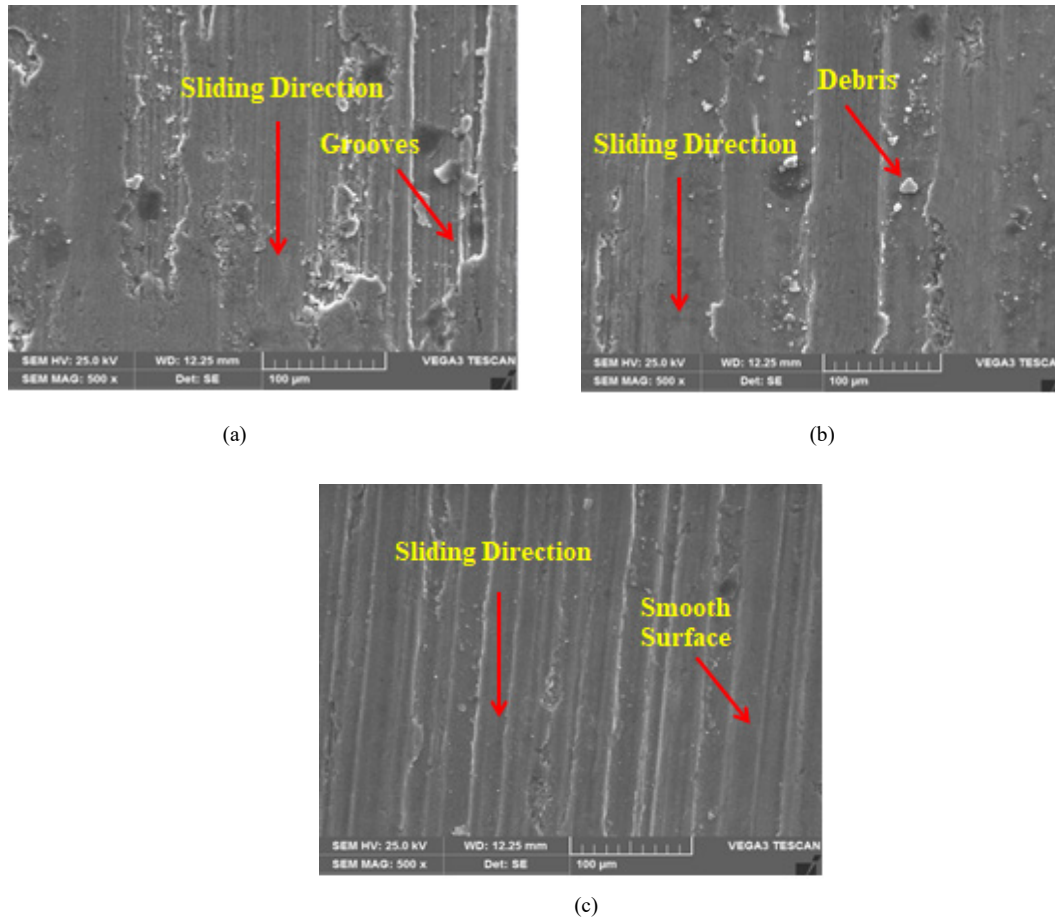


Figure 7. Worn surfaces SEM of (a) Al2219 material (b) Al2219 with 2 wt. % B_4C (c) Al2219 with 4 wt. % B_4C composites.

5.0 References

1. Dhanesh S. Materials today: Proceedings. 2021; 45(2):1376-81. <https://doi.org/10.1016/j.matpr.2020.06.325>
2. Kumar HS *et al.* Journal of Failure Analysis and Prevention. 2021; 21(6):2177-89. <https://doi.org/10.1007/s11668-021-01265-w>
3. Rajmohan T *et al.*, Transactions of Nonferrous Metals Society of China. 2013; 23:2509-17. [https://doi.org/10.1016/S1003-6326\(13\)62762-4](https://doi.org/10.1016/S1003-6326(13)62762-4)
4. Veereshkumar GB *et al.* Composites Part B: Engineering. 2019; 175:107138. <https://doi.org/10.1016/j.compositesb.2019.107138>
5. Siddesh Kumar NG *et al.* Measurement. 2017; 107:1-11. <https://doi.org/10.1016/j.measurement.2017.05.003>
6. Jadhav PR *et al.* Advanced Composites and Hybrid Materials. 2020; 3:114-9. <https://doi.org/10.1007/s42114-020-00143-7>
7. Wang RM *et al.* Materials Science and Engineering A. 1998; 254:219-26. [https://doi.org/10.1016/S0921-5093\(98\)00686-8](https://doi.org/10.1016/S0921-5093(98)00686-8)
8. Harti JI *et al.* American Journal of Materials Science. 2015; 5(3C):34-7.
9. Kalaiselvan K *et al.* Materials and Design. 2011; 32:4004-9. <https://doi.org/10.1016/j.matdes.2011.03.018>
10. Patidar D *et al.* Materials Today Proceedings. 2017; 4:2981-8. <https://doi.org/10.1016/j.matpr.2017.02.180>
11. Matti S *et al.* Indian Journal of Science and Technology. 2021; 14(4):310-8. <https://doi.org/10.17485/IJST/v14i4.2081>
12. Rajmohan T *et al.* Transactions of Nonferrous Metals Society of China. 2013; 23:2509-17. [https://doi.org/10.1016/S1003-6326\(13\)62762-4](https://doi.org/10.1016/S1003-6326(13)62762-4)